

# Preference-based Centrality and Ranking in General Metric Spaces

Lingfeng Lyu<sup>1,2</sup>, Doudou Zhou<sup>1\*</sup>

<sup>1</sup> Department of Statistics and Data Science, National University of Singapore

<sup>2</sup> Department of Statistics and Finance, University of Science and Technology of China

## Abstract

Assessing centrality or ranking observations in multivariate or non-Euclidean spaces is challenging because such data lack an intrinsic order and many classical depth notions lose resolution in high-dimensional or structured settings. We propose a preference-based framework that defines centrality through population pairwise proximity comparisons: a point is central if a typical draw from the underlying distribution tends to lie closer to it than to another. This perspective yields a well-defined statistical functional that generalizes data depth to arbitrary metric spaces. To obtain a coherent one-dimensional representation, we study a Bradley–Terry–Luce projection of the induced preferences and develop two finite-sample estimators based on convex M-estimation and spectral aggregation. The resulting procedures are consistent, scalable, and applicable to high-dimensional and non-Euclidean data, and across a range of examples they exhibit stable ranking behavior and improved resolution relative to classical depth-based methods.

*Keywords:* multivariate ranking; statistical depth; pairwise comparison; Bradley–Terry–Luce model; general metric spaces

---

\*Corresponding author: ddzhou@nus.edu.sg

# 1 Introduction

Centrality is a fundamental concept in statistics and the applied sciences. It underlies representative point selection, outlier detection, risk stratification, and the construction of interpretable orderings. In univariate settings, the real line provides a canonical order, so centrality and ranking are naturally defined through ranks, quantiles, and order statistics. In contrast, modern data are frequently multivariate or live on non-Euclidean spaces such as manifolds, networks, graphs, and learned embedding spaces, where no intrinsic notion of order is available. In these settings, defining population-level centrality and estimating a stable, interpretable ordering from finite samples remain challenging problems.

A broad literature has sought to generalize ranking and centrality beyond the univariate case. Classical approaches include componentwise and spatial ranks (Hallin and Puri, 1995; Puri and Sen, 1966; Chaudhuri, 1996; Oja, 2010), depth-induced orderings (Liu and Singh, 1993; Zuo and Serfling, 2000), Mahalanobis and metric-based constructions (Hallin and Paindaveine, 2002, 2006; Pan et al., 2018), and more recent transport- or graph-based formulations (Deb and Sen, 2023; Zhou and Chen, 2023). Statistical depth, in particular, has emerged as a principled framework for multivariate centrality, formalizing center-outward ordering through axioms such as affine equivariance, maximality, monotonicity, and robustness (Tukey, 1974; Liu, 1990; Vardi and Zhang, 2000; Zuo, 2003; Parzen, 1962). Despite their success, many existing depth notions rely on linear or convex structure and can lose discriminative power or become computationally burdensome in high dimensions or in complex geometries, where distance concentration, hubness, and anisotropy obscure purely geometric notions of centrality (Radovanovic et al., 2010; Feldbauer and Flexer, 2019). More broadly, when only a general dissimilarity is available, it is often unclear what population object a given surrogate score targets, and how pairwise information across the sample should be coherently aggregated into a global ordering.

This paper takes a different starting point. Rather than constructing centrality directly from global geometric summaries, we ground it in *reference-based pairwise comparisons*. Given two candidates, we ask which one tends to be closer to a typical draw from the underlying distribution. Such comparisons are intrinsic, require only a dissimilarity measure, and remain well-defined on arbitrary metric spaces. Formally, let  $F$  be a probability measure on a space  $\mathcal{X}$  equipped with a measurable dissimilarity function  $\delta : \mathcal{X} \times \mathcal{X} \rightarrow [0, \infty)$ .

We define the population preference

$$p_F(x, y) = \mathbb{P}_{Z \sim F}\{\delta(Z, x) > \delta(Z, y)\},$$

and the induced centrality functional

$$r_F(y) = \mathbb{E}_{X \sim F}[p_F(X, y)]. \quad (1)$$

Intuitively,  $r_F(y)$  is the probability that  $y$  “wins” against a random opponent when judged by a random reference point. This functional provides a natural, population-level notion of centrality that is defined solely in terms of  $(F, \delta)$  and applies equally to Euclidean, high-dimensional, and non-Euclidean data.

Estimating and using  $r_F(\cdot)$  in practice, however, raises two fundamental challenges. First, the induced pairwise preferences need not be transitive: it is possible to have  $x$  preferred to  $y$ ,  $y$  preferred to  $z$ , and  $z$  preferred to  $x$ , even at the population level. Second, empirical estimates of  $p_F(x, y)$  are noisy and strongly dependent, as they are constructed from shared reference points. As a result, naive aggregation schemes, such as empirical win rates, can yield unstable rankings and provide limited inferential structure.

To address these issues, we propose to aggregate induced preferences through a calibrated one-dimensional projection. Specifically, we consider a Bradley–Terry–Luce (BTL) type representation (Bradley and Terry, 1952; Luce, 1959) that maps pairwise preferences onto a transitive score scale by minimizing a population cross-entropy risk. Importantly, this formulation is used as a *projection* rather than as a correctly specified model: the resulting score function is defined as the unique minimizer of a well-posed M-estimation problem and exists regardless of whether the BTL form exactly matches the underlying preference probabilities. This projection enforces global coherence of the ordering, regularizes noisy comparisons, and yields interpretable log-odds scores that support efficient computation and principled out-of-sample evaluation.

We call the resulting framework CORE (Centrality Ordering via Relative Evaluation). At the population level, we show that the calibrated score is a strictly monotone transformation of  $r_F(\cdot)$ , ensuring that the projection preserves the intrinsic preference-based ordering while providing a stable and interpretable coordinate system. At the sample level, we develop two complementary estimators: a convex optimization-based estimator and a fast spectral estimator based on the stationary distribution of an empirical comparison

operator. We establish identifiability, consistency, and stability of the proposed scores under mild conditions, and show that, in settings where such structure is available, the induced population score satisfies the canonical center–outward properties associated with statistical depth. Through simulations and real-data analyses, we demonstrate that CORE yields sharper discrimination and more stable rankings than direct win-rate aggregation and widely used depth-based methods, particularly in high-dimensional and non-Euclidean settings.

The remainder of the paper is organized as follows. Section 2 introduces the CORE framework and the proposed estimators. Section 3 develops the theoretical properties of the population and sample-level scores. Section 4 presents simulation studies. Section 5 concludes with a discussion and directions for future work.

## 2 Method

### 2.1 From induced preferences to a calibrated centrality score

The population preference function  $p_F(\cdot, \cdot)$  encodes reference-based pairwise comparisons induced by  $(F, \delta)$ . While these comparisons are intrinsic and well-defined on general dissimilarity spaces,  $p_F$  is a bivariate object and does not directly yield a scalar notion of centrality or a coherent global ordering on  $\mathcal{X}$ . In particular, the induced majority relation  $x \succ y$  defined by  $p_F(y, x) > 1/2$  need not be transitive and may exhibit preference cycles, even at the population level; see Supplementary S.1 for an explicit example. These features motivate aggregating pairwise preferences through a calibrated one-dimensional representation that enforces global coherence while retaining the intrinsic comparison structure.

We adopt a BTL type formulation as a projection device. Let  $\theta : \mathcal{X} \rightarrow \mathbb{R}$  be a real-valued score function and define

$$q_\theta(x, y) = \frac{\exp\{\theta(y)\}}{\exp\{\theta(x)\} + \exp\{\theta(y)\}}, \quad x, y \in \mathcal{X}. \quad (2)$$

Larger values of  $\theta(\cdot)$  correspond to higher centrality, and the induced ordering is transitive by construction. Importantly, we do not assume that  $q_\theta$  correctly specifies the true preference probabilities  $p_F$ . Instead, the BTL form is used as a calibrated projection that maps possibly cyclic preferences onto a coherent score scale.

We formalize this projection through a population M-estimation problem. Specifically, we quantify the discrepancy between  $p_F$  and  $q_\theta$  using the cross-entropy risk

$$\mathcal{L}_F(\theta) = \mathbb{E}_{X,Y \sim F} [-p_F(X, Y) \log q_\theta(X, Y) - \{1 - p_F(X, Y)\} \log\{1 - q_\theta(X, Y)\}]. \quad (3)$$

Since  $q_\theta(x, y)$  depends only on score differences  $\theta(y) - \theta(x)$ , the risk  $\mathcal{L}_F(\theta)$  is invariant under additive shifts of  $\theta$ . To ensure identifiability, we work with centered score functions. Let  $L_0^2(F) = \{\theta \in L^2(F) : \mathbb{E}_F[\theta(X)] = 0\}$  and let  $\Theta(F) \subset L^2(F)$  be a user-specified function class. We define  $\Theta_0(F) = \Theta(F) \cap L_0^2(F)$  and set

$$\theta^* \in \operatorname{argmin}_{\theta \in \Theta_0(F)} \mathcal{L}_F(\theta). \quad (4)$$

The resulting  $\theta^*$  is a population-level calibrated centrality score. For convenience, we also define the associated strength function  $s^*(x) = \exp\{\theta^*(x)\}$ , which induces the same ordering as  $\theta^*$ .

## 2.2 Sample-level M-estimation of centrality scores

Let  $x_1, \dots, x_n$  be an i.i.d. sample from  $F$ . Rather than imposing additional structure on  $\theta(\cdot)$ , we adopt a fully nonparametric sample-level formulation by estimating the score function only at the observed data points. Specifically, we seek to estimate the score vector  $\boldsymbol{\theta} = (\theta_1, \dots, \theta_n)^\top$ , where  $\theta_i$  represents  $\theta(x_i)$ .

Under the BTL projection (2), the probability that  $x_j$  is preferred to  $x_i$  is given by  $q_\theta(x_i, x_j) = \sigma(\theta_j - \theta_i)$ , where  $\sigma(t) = (1 + e^{-t})^{-1}$ . Replacing population quantities in (3) with empirical counterparts yields the sample objective

$$\mathcal{L}_n(\boldsymbol{\theta}) = \sum_{1 \leq i < j \leq n} \left[ -\hat{p}_{ij} \log \sigma(\theta_j - \theta_i) - (1 - \hat{p}_{ij}) \log\{1 - \sigma(\theta_j - \theta_i)\} \right], \quad (5)$$

where  $\hat{p}_{ij}$  denotes an empirical estimator of  $p_F(x_i, x_j)$ . As in the population case, the objective is invariant under global shifts of  $\boldsymbol{\theta}$ , and we impose the centering constraint  $\mathbf{1}^\top \boldsymbol{\theta} = 0$ . The estimator is defined as

$$\hat{\boldsymbol{\theta}} = \operatorname{argmin}_{\boldsymbol{\theta} \in \mathbb{R}^n, \mathbf{1}^\top \boldsymbol{\theta} = 0} \mathcal{L}_n(\boldsymbol{\theta}). \quad (6)$$

We solve (6) using projected first-order optimization; Algorithm 1 summarizes the procedure. The estimated strength scores are  $\hat{s}_i = \exp(\hat{\theta}_i)$ , and the sample preference center is defined as  $\hat{\mu} = x_{\hat{i}}$  with  $\hat{i} \in \operatorname{argmax}_i \hat{\theta}_i$ .

**A fast spectral approximation.** For large  $n$ , directly solving (6) can be computationally demanding. As a scalable alternative, we consider a spectral approximation that is closely related to classical spectral ranking methods for paired comparisons (Negahban et al., 2017). Given the empirical preference matrix  $\{\hat{p}_{ij}\}$ , we construct a Markov transition matrix  $\mathbf{T} = [T_{ij}]_{i,j=1}^n$  defined by

$$T_{ij} = \frac{1}{n-1} \hat{p}_{ij} \mathbb{I}(i \neq j) + \left(1 - \frac{1}{n-1} \sum_{k \neq i} \hat{p}_{ik}\right) \mathbb{I}(i = j).$$

This construction induces a random walk that, at each step, moves from state  $i$  to state  $j$  with probability proportional to the probability that  $j$  is preferred to  $i$ . The stationary distribution  $\hat{\mathbf{s}}$  of  $\mathbf{T}$  (i.e., the probability vector satisfying  $\hat{\mathbf{s}} = \mathbf{T}^\top \hat{\mathbf{s}}$ ) provides a strength score that serves as a spectral approximation to the BTL M-projection, in the sense that it replaces the global convex optimization in (6) with a linear eigenvector computation while preserving the same underlying preference aggregation structure. Centering the logarithm of  $\hat{\mathbf{s}}$  yields an approximate solution to (6). Algorithm 2 details the implementation. For faster computation, we also implement a quasi-Newton solver based on L-BFGS-B updates; the corresponding procedure is provided in Supplementary Section S.2 (Algorithm S.1).

### 2.3 Construction of empirical pairwise preferences

Both estimators require empirical pairwise preferences  $\hat{p}_{ij}$ . Our primary construction is the leave-two-out estimator

$$\hat{p}_{ij}^{\text{lt}} = \frac{1}{n-2} \sum_{\ell \neq i,j} \mathbb{I}\{\delta(x_\ell, x_i) > \delta(x_\ell, x_j)\}, \quad (7)$$

which uses all available observations as reference points. This estimator is statistically efficient but induces dependence across entries of the preference matrix.

For theoretical analysis and uncertainty quantification, we also consider a data-reference estimator based on an independent sample  $Z_1, \dots, Z_m \stackrel{\text{i.i.d.}}{\sim} F$ :

$$\hat{p}_{ij}^{\text{ref}} = \frac{1}{m} \sum_{l=1}^m \mathbb{I}\{\delta(Z_l, x_i) > \delta(Z_l, x_j)\}. \quad (8)$$

Finally, sample splitting can be used to ensure conditional independence of the summands at the cost of evaluating centrality only on a subset of points.

---

**Algorithm 1** CORE-GD: M-estimation via projected first-order optimization

---

**Input:** pairwise preference matrix  $\mathbf{P} = \{\hat{p}_{ij}\}_{1 \leq i, j \leq n}$ , stepsize  $\eta > 0$ , tolerance  $\varepsilon > 0$ , maximum iteration  $T_{\max}$ .

**Initialize:**  $\boldsymbol{\theta}^{(0)} \leftarrow \mathbf{0} \in \mathbb{R}^n$ .

**For**  $t = 0, 1, \dots, T_{\max} - 1$ :

- Compute the gradient of  $\mathcal{L}_n$  at  $\boldsymbol{\theta}^{(t)}$ :

$$\mathbf{g}^{(t)} = \sum_{1 \leq i < j \leq n} (\sigma(\theta_j^{(t)} - \theta_i^{(t)}) - \hat{p}_{ij}) (\mathbf{e}_j - \mathbf{e}_i).$$

- Enforce the centering constraint by projecting the gradient:

$$\mathbf{g}^{(t)} \leftarrow \mathbf{g}^{(t)} - \frac{\mathbf{1}^\top \mathbf{g}^{(t)}}{n} \mathbf{1}.$$

- Update:  $\boldsymbol{\theta}^{(t+1)} \leftarrow \boldsymbol{\theta}^{(t)} - \eta \mathbf{g}^{(t)}$ .

- Stop if  $\|\mathbf{g}^{(t)}\|_\infty \leq \varepsilon$ .

**Output:**  $\hat{\boldsymbol{\theta}} = \boldsymbol{\theta}^{(t)}$ .

---

---

**Algorithm 2** CORE-Spectral: spectral scores via the stationary distribution

---

**Input:** pairwise preference matrix  $\mathbf{P} = \{\hat{p}_{ij}\}_{i, j=1}^n$  with  $\hat{p}_{ii} = 0$ , tolerance  $\varepsilon > 0$ , maximum iterations  $T_{\max}$ .

**Step I (Transition matrix).** Construct  $\mathbf{T} = [T_{ij}]_{i, j=1}^n$  by

$$T_{ij} = \frac{1}{n-1} \hat{p}_{ij} \mathbb{I}(i \neq j) + \left(1 - \frac{1}{n-1} \sum_{k \neq i} \hat{p}_{ik}\right) \mathbb{I}(i = j).$$

**Step II (Power iteration).** Initialize  $\mathbf{s}^{(0)} = \frac{1}{n} \mathbf{1}$ . For  $t = 0, 1, \dots, T_{\max} - 1$ , iterate

$$\mathbf{s}^{(t+1)} = \mathbf{T}^\top \mathbf{s}^{(t)}.$$

Stop if  $\|\mathbf{s}^{(t+1)} - \mathbf{s}^{(t)}\|_1 \leq \varepsilon$ , and set  $\hat{\mathbf{s}} = \mathbf{s}^{(t+1)}$ .

**Step III (Centered log-scores).** Let  $\hat{s}_i$  denote the  $i$ th entry of  $\hat{\mathbf{s}}$  and define

$$\hat{\theta}_i = \log \hat{s}_i - \frac{1}{n} \sum_{k=1}^n \log \hat{s}_k, \quad i = 1, \dots, n.$$

**Output:**  $\hat{\mathbf{s}} = (\hat{s}_1, \dots, \hat{s}_n)^\top$  and  $\hat{\boldsymbol{\theta}} = (\hat{\theta}_1, \dots, \hat{\theta}_n)^\top$ .

---

## 2.4 Out-of-sample scoring

To extend the fitted scores beyond the observed sample, we employ kernel smoothing on the dissimilarity space. Given a kernel  $K : [0, \infty) \rightarrow [0, \infty)$  and bandwidth  $h > 0$ , we define weights

$$w_i(x) = \frac{K(\delta(x, x_i)/h)}{\sum_{k=1}^n K(\delta(x, x_k)/h)}, \quad i = 1, \dots, n, \quad (9)$$

and set

$$\hat{\theta}(x) = \sum_{i=1}^n w_i(x) \hat{\theta}_i, \quad \hat{s}(x) = \exp\{\hat{\theta}(x)\}. \quad (10)$$

This construction can be viewed as a Nadaraya–Watson-type extension on  $(\mathcal{X}, \delta)$ . In practice, we use the Gaussian kernel  $K(t) = \exp(-t^2)$  and set  $h$  to the median pairwise distance among the sample points.

**Remark 1** (Discrete scores versus parametric scoring). *At the population level, the centrality score  $\theta^*(\cdot)$  is defined as a function on  $\mathcal{X}$  through the M-projection in (4). At the sample level, we adopt a fully nonparametric formulation by estimating this score only at the observed data points, yielding a finite-dimensional vector  $\hat{\theta} = (\hat{\theta}_1, \dots, \hat{\theta}_n)^\top$ .*

*This discretized estimation strategy avoids imposing additional structural assumptions on  $\theta(\cdot)$  and aligns with classical depth- and rank-based constructions, which define population functionals but operate on sample-level scores. Out-of-sample values are subsequently obtained through smoothing, as described in Section 2.4.*

*An alternative approach is to estimate  $\theta(\cdot)$  directly within a parametric or reproducing kernel class from reference-based comparisons. Recent trainable centrality and ranking frameworks pursue this direction; see, for example, Vu et al. (2025). We view such parametric approaches as complementary, offering amortized out-of-sample scoring at the cost of additional modeling assumptions.*

**Remark 2** (Win-rate scores and their relation to CORE). *A direct sample analog of (1) is the average win rate*

$$\hat{r}_j := \frac{1}{n-1} \sum_{i \neq j} \hat{p}_{ij}, \quad j = 1, \dots, n,$$

*which can be viewed as the average win probability of  $x_j$  against a randomly chosen opponent. Theorem 2 shows that, at the population level, the M-projection score  $\theta^*(\cdot)$  is a*

strictly monotone transform of  $r(\cdot)$ . As a result,  $\hat{r}_j$  and  $\hat{\theta}_j$  induce aligned one-dimensional orderings in large samples.

However, the BTL projection provides a calibrated score representation that enforces global coherence of the ordering, regularizes noisy pairwise comparisons, and yields interpretable log-odds differences, which are not available from raw win rates.

### 3 Theoretical Properties

This section studies the population properties of the calibrated centrality score  $\theta^*$  defined through the M-projection in (4). Our analysis proceeds in three steps. First, we establish that the population projection problem is well-posed and admits a unique solution. Second, we show that the resulting score is intrinsically linked to the preference-based centrality functional  $r(\cdot)$  through a monotone transformation, independently of correct model specification. Finally, we demonstrate that the induced population score satisfies the canonical axioms of statistical depth and recovers familiar center–outward orderings in symmetric benchmark settings.

#### 3.1 Existence and uniqueness of the centered minimizer

We begin by showing that the population M-projection defining  $\theta^*$  is well-defined. Since the optimization is carried out over a space of functions, mild regularity conditions are required to ensure existence and identifiability of the solution.

**Assumption 1** (Centered parameter class). *The centered class  $\Theta_0(F)$  is nonempty, convex, and compact in  $L^2(F)$ .*

Assumption 1 is standard in functional M-estimation. Convexity rules out multiple local optima, while compactness guarantees existence of a minimizer in the infinite-dimensional function space.

**Theorem 1** (Existence and uniqueness). *Under Assumption 1, the risk functional  $\mathcal{L}_F$  defined in (3) has a unique minimizer over  $\Theta_0(F)$ .*

Theorem 1 ensures that the M-projection problem admits a unique population solution  $\theta^* \in \Theta_0(F)$ . This result identifies a single, well-defined calibrated score function that serves as the population target of the proposed methodology.

**Remark 3** (Correct specification as a special case). *If the working BTL model happens to be correctly specified, so that  $p_F(X, Y) = q_{\theta^*}(X, Y)$  almost surely, then  $\theta^*$  coincides with the true underlying score function. In this case, the M-projection reduces to the usual likelihood-based identification, with the centering constraint selecting a unique representative among shift-equivalent solutions.*

### 3.2 A monotone link between calibrated scores and preference centrality

The existence and uniqueness result above ensures that the calibrated score  $\theta^*$  is well-defined. We now show that this score is intrinsically linked to the preference-based centrality functional  $r(\cdot)$  introduced in Section 1. Importantly, this link holds without assuming correct specification of the BTL working model.

**Theorem 2** (Monotone calibration link between  $\theta^*$  and  $r$ ). *Suppose Assumption 1 holds and that  $\theta^*$  lies in the relative interior of  $\Theta_0(F)$ . Define*

$$H(t) := \mathbb{E}_{X \sim F} [\sigma\{t - \theta^*(X)\}], \quad t \in \mathbb{R}.$$

*Then  $H : (-\infty, \infty) \rightarrow (0, 1)$  is strictly increasing and satisfies*

$$H(\theta^*(y)) = r(y) \quad \text{for } F\text{-a.e. } y \in \mathcal{X}. \quad (11)$$

*In particular,  $\theta^*(\cdot)$  is a strictly monotone transformation of  $r(\cdot)$ , and*

$$\theta^*(y) = H^{-1}(r(y)) \quad \text{for } F\text{-a.e. } y \in \mathcal{X},$$

*where  $H^{-1}$  denotes the inverse of  $H$  on its range.*

Theorem 2 establishes that the calibrated score  $\theta^*(\cdot)$  is a strictly monotone reparameterization of the preference centrality  $r(\cdot)$ . As a consequence,  $\theta^*$  and  $r$  induce identical population orderings up to  $F$ -null sets, and the M-projection preserves the intrinsic preference structure while mapping it onto a coherent one-dimensional scale.

The relative-interior condition is a mild technical assumption ensuring that first-order optimality conditions characterize the solution of the constrained optimization problem. It rules out boundary solutions at which only restricted perturbations are admissible.

### 3.3 Depth properties of the M-projection scores

While  $\theta^*(\cdot)$  provides a calibrated ranking, it is natural to ask whether the induced strength score  $s^*(\cdot) = \exp\{\theta^*(\cdot)\}$  admits a genuine center–outward interpretation. We answer this question by showing that, under mild regularity conditions,  $s^*$  satisfies the four canonical axioms of statistical depth (Zuo and Serfling, 2000).

**Assumption 2** (Center–outward regularity of preference centrality). *Assume that the preference-based centrality functional  $r(\cdot)$  satisfies the following population-level regularity conditions.*

(A1) *Affine equivariance. For any invertible matrix  $A$  and vector  $b$ , define the affine transformation  $T_{A,b}(x) = Ax + b$  and let  $G = T_{A,b}\#F$  denote the pushforward distribution. The induced preferences are equivariant in the sense that*

$$p_G(T_{A,b}x, T_{A,b}y) = p_F(x, y) \quad \text{for all } x, y \in \mathcal{X},$$

*and the centered parameter class transforms accordingly as*

$$\Theta_0(G) = \{\theta \circ T_{A,b}^{-1} : \theta \in \Theta_0(F)\}.$$

(A2) *Existence of a preference center and center–outward monotonicity. There exists at least one maximizer  $\mu \in \arg \max_{y \in \mathcal{X}} r(y)$  such that for any  $x \in \mathcal{X}$  and any  $\alpha \in [0, 1]$ , the interpolated point  $x_\alpha = (1 - \alpha)\mu + \alpha x$  satisfies*

$$r(x_\alpha) \geq r(x).$$

*When  $\arg \max r$  is not a singleton, we fix any maximizer  $\mu$  satisfying this property.*

(A3) *Vanishing of centrality at infinity. Let  $Z \sim F$ . For any sequence  $(y_m)$  with  $\delta(y_m, \mu) \rightarrow \infty$  and any fixed radius  $M > 0$ ,*

$$\mathbb{P}\{\delta(y_m, Z) \leq M\} \rightarrow 0,$$

*so that points arbitrarily far from the center have asymptotically negligible preference centrality.*

Assumption 2 imposes population-level center–outward regularity on the preference centrality functional  $r(\cdot)$ . Collectively, conditions (A1)–(A3) mirror the canonical depth axioms of Zuo and Serfling (2000): affine equivariance, maximality at a center, monotonicity toward the center, and vanishing at infinity. Via the monotone link in Theorem 2, these properties transfer directly from  $r(\cdot)$  to the CORE score  $s^*(\cdot)$ .

**Theorem 3** (Depth properties). *Suppose Assumptions 1 and 2 hold and that  $\theta^*$  lies in the relative interior of  $\Theta_0(F)$ . Then  $s^*(x) = \exp\{\theta^*(x)\}$  satisfies the four canonical depth axioms:*

(D1) **Affine invariance.** For  $G = T_{A,b}\#F$ ,

$$s_G^*(T_{A,b}x) = s^*(x).$$

(D2) **Maximality at the center.** If  $\mu$  is as in Assumption 2(A2), then  $s^*(\mu) \geq s^*(x)$  for all  $x$ .

(D3) **Monotonicity toward the deepest point.** For  $x_\alpha = (1-\alpha)\mu + \alpha x$  with  $\alpha \in [0, 1]$ ,

$$s^*(x_\alpha) \geq s^*(x).$$

(D4) **Vanishing at infinity.** If  $\delta(y_m, \mu) \rightarrow \infty$ , then  $s^*(y_m) \rightarrow 0$ .

Theorem 3 provides an axiomatic characterization of the CORE population score  $s^*$  as a statistical depth function. While depth axioms describe qualitative behavior, it is also instructive to examine the explicit form of  $\theta^*$  in symmetric benchmark models.

### 3.3.1 One-dimensional symmetric distribution

We begin with the one-dimensional Euclidean setting  $\mathcal{X} = \mathbb{R}$ . In this case, symmetry about a center  $\mu$  suggests that any reasonable population centrality should assign equal importance to  $\mu + t$  and  $\mu - t$  and depend on  $x$  only through its deviation from the center. This intuition underlies classical univariate depth notions and motivates the reflection-symmetry assumption below.

**Assumption 3** (Reflection symmetry). *Assume  $\mathcal{X} = \mathbb{R}$  and  $\delta(x, y) = |x - y|$ . Assume that for  $X \sim F$ ,*

$$X - \mu \stackrel{d}{=} \mu - X,$$

*so that  $F$  is symmetric about  $\mu$ .*

**Proposition 1.** Suppose the conditions of Theorem 2 are satisfied and Assumption 3 holds. Then there exists a function  $\varphi: [0, \infty) \rightarrow \mathbb{R}$  such that

$$\theta^*(x) = \varphi(|x - \mu|), \quad x \in \mathbb{R}.$$

If in addition Assumption 2(A2) holds, then  $\varphi$  can be chosen non-increasing. In particular, if  $|x - \mu| < |y - \mu|$ , then  $\theta^*(x) \geq \theta^*(y)$ .

Proposition 1 shows that, under reflection symmetry, the calibrated population score depends only on the distance to the center and decreases monotonically as one moves away from  $\mu$ . Consequently,  $\theta^*$  is maximized at the symmetry center  $\mu$  and induces the canonical one-dimensional center–outward ordering. Importantly, this structural characterization holds regardless of whether the BTL working model correctly specifies the underlying preference probabilities, demonstrating that the proposed calibration preserves the intrinsic geometry implied by distributional symmetry.

### 3.3.2 Multivariate elliptically symmetric distribution

We next consider the multivariate Euclidean setting  $\mathcal{X} = \mathbb{R}^d$  under elliptical symmetry. In this setting, the geometry of the distribution is characterized by a location parameter  $\mu$  and a positive definite scatter matrix  $\Sigma$ , and centrality is naturally described in terms of distances measured relative to  $\Sigma$ . Classical multivariate depth constructions, most notably Mahalanobis depth, exploit this structure to induce center–outward orderings based on ellipsoidal level sets.

To make this connection precise, we equip  $\mathcal{X}$  with the Mahalanobis dissimilarity associated with  $\Sigma$  and formalize elliptical symmetry through an invariance condition in whitened coordinates.

**Assumption 4.** Assume  $\mathcal{X} = \mathbb{R}^d$  and equip it with the Mahalanobis dissimilarity

$$\delta_\Sigma(x, y) := \{(x - y)^\top \Sigma^{-1} (x - y)\}^{1/2}, \quad \Sigma \in \mathbb{R}^{d \times d} \text{ positive definite.}$$

Assume that for  $X \sim F$  and every orthogonal matrix  $O$ ,

$$\Sigma^{-1/2}(X - \mu) \stackrel{d}{=} O \Sigma^{-1/2}(X - \mu),$$

which characterizes elliptical symmetry of  $F$  about  $\mu$  with scatter matrix  $\Sigma$ .

**Proposition 2.** Suppose the conditions of Theorem 2 are satisfied and Assumption 4 holds. Then there exists a function  $\varphi: [0, \infty) \rightarrow \mathbb{R}$  such that

$$\theta^*(x) = \varphi(\delta_\Sigma(x, \mu)), \quad x \in \mathbb{R}^d.$$

If in addition Assumption 2(A2) holds, then  $\varphi$  can be chosen non-increasing. In particular, if  $\delta_\Sigma(x, \mu) < \delta_\Sigma(y, \mu)$ , then  $\theta^*(x) \geq \theta^*(y)$ .

Proposition 2 shows that, under elliptical symmetry, the CORE population score induces the same center–outward ordering as classical Mahalanobis depth. Specifically, the induced centrality score is constant on ellipsoids centered at  $\mu$  with shape matrix  $\Sigma$  and decreases monotonically with the Mahalanobis radius  $\delta_\Sigma(x, \mu)$ . Consequently, the score is maximized at the location parameter  $\mu$  and recovers the canonical multivariate center–outward ordering characteristic of Mahalanobis depth. This confirms that our framework correctly adapts to the underlying covariance structure, effectively accounting for the geometry encoded by  $\Sigma$  to recover the intrinsic notion of multivariate centrality.

## 4 Simulation Studies

This section investigates the finite-sample behavior of the proposed CORE estimators under Euclidean geometry. The simulations are designed to address two complementary questions. First, in a one-dimensional setting where the population preference structure is analytically tractable, we examine how the estimated score functions converge as the sample size increases and compare the gradient-based and spectral implementations. Second, in moderate and high dimensions, we evaluate the ability of CORE to recover the population benchmark ranking induced by the preference centrality  $r_F(\cdot)$  and contrast its performance with classical depth-based procedures.

### 4.1 One-dimensional score convergence

We begin with a one-dimensional setting in which the population preference function  $p_F(\cdot, \cdot)$  admits a closed-form expression. This allows us to directly visualize the estimated score functions and assess their convergence toward the population target as the sample size increases.

We consider sample sizes  $n \in \{50, 200, 500, 2000\}$  with  $R = 20$  independent replications for each  $n$ . In each replication, we generate  $x_1, \dots, x_n \stackrel{\text{i.i.d.}}{\sim} F$ , where  $F$  is either (i) the standard normal distribution  $N(0, 1)$ , or (ii) a skewed Laplace distribution with density

$$f(x) = \frac{1}{b_L + b_R} \{ \exp(x/b_L) \mathbf{1}(x < 0) + \exp(-x/b_R) \mathbf{1}(x \geq 0) \},$$

with  $(b_L, b_R) = (2, 1)$ . The dissimilarity is set to  $\delta(x, y) = |x - y|$ .

We compare three constructions of the pairwise preference matrix. First, we consider the *population* matrix  $\mathbf{P} = \{p_{ij}\}$  with  $p_{ij} = p_F(x_i, x_j)$ . In one dimension, letting  $F_{\text{cdf}}$  denote the distribution function of  $F$ , the preference probability admits the closed form

$$p_F(x_i, x_j) = \begin{cases} 1 - F_{\text{cdf}}((x_i + x_j)/2), & x_i < x_j, \\ F_{\text{cdf}}((x_i + x_j)/2), & x_i > x_j. \end{cases}$$

Second, we use the independent *reference-sample* estimator  $\mathbf{P}^{\text{ref}} = \{\hat{p}_{ij}^{\text{ref}}\}$  defined in (8), computed from an independent sample  $Z_1, \dots, Z_n \stackrel{\text{i.i.d.}}{\sim} F$ . Third, we consider the *leave-two-out* estimator  $\mathbf{P}^{\text{lto}} = \{\hat{p}_{ij}^{\text{lto}}\}$  in (7), which uses the observed sample itself as reference points.

For each preference matrix, we compute the corresponding score vector using the gradient-based implementation (Algorithm 1), referred to as *Population-GD*, *Reference-GD*, and *Leave-out-GD*, respectively. In addition, we apply the spectral estimator (Algorithm 2) to  $\mathbf{P}^{\text{lto}}$ , yielding the *Leave-out-Spectral* estimator.

Figure 1 overlays the four estimated score curves obtained from the same dataset for each combination of distribution and sample size. As  $n$  increases, the three gradient-based estimators become nearly indistinguishable, indicating that the leave-two-out and reference constructions recover the same limiting score as the population benchmark. The spectral estimator exhibits slightly larger deviations in the tails, but induces essentially the same ordering.

Figure 2 fixes the distribution and estimation method and overlays the score curves across different sample sizes. For all methods, the curves stabilize toward a common limiting shape as  $n$  grows. The vertical dashed line marks the population maximizer  $\mu^*$  of  $r(\cdot)$  ( $\mu^* = 0$  for the normal distribution and  $\mu^* = -0.462$  for the skewed Laplace case). Even for moderate sample sizes, the estimated scores peak near  $\mu^*$ , demonstrating reliable recovery of the population center.

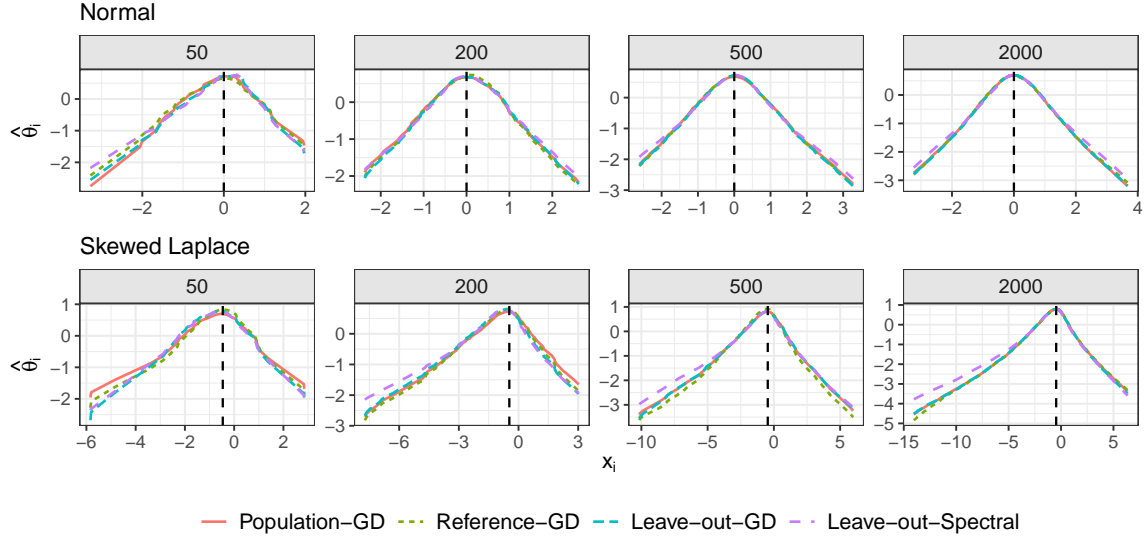


Figure 1: One-dimensional comparison of four CORE estimators. Each panel corresponds to a distribution (Normal or skewed Laplace) and a sample size  $n \in \{50, 200, 500, 2000\}$ . Estimated scores  $\hat{\theta}_i$  are plotted against the sample points  $x_i$ . The vertical dashed line marks the population maximizer  $\mu^*$  of  $r(\cdot)$ .

Figure 3 reports the mean Pearson correlation between each estimated score vector and the Population-GD benchmark across  $R = 20$  replications. As  $n$  increases, correlations for all methods approach one and the variability across replications diminishes. Notably, the gap between Reference-GD and Leave-out-GD narrows rapidly with  $n$ , indicating that the leave-two-out estimator achieves comparable accuracy without requiring an additional independent reference sample. The spectral estimator remains slightly less correlated than the gradient-based methods, but consistently exhibits high agreement with the population benchmark.

## 4.2 Rank recovery in moderate and high dimensions

We next study the ability of CORE and competing procedures to recover the population ranking induced by the preference-based centrality functional  $r_F(\cdot)$  under the Euclidean dissimilarity  $\delta(x, y) = \|x - y\|_2$ , in moderate to high dimensions. We consider four  $(n, d)$  configurations:  $(150, 80)$  and  $(500, 200)$  representing the  $n > d$  regime, and  $(80, 200)$  and  $(150, 500)$  representing the high-dimension, low-sample-size regime  $n < d$ . For each configuration, results are averaged over  $R = 20$  independent replicates.

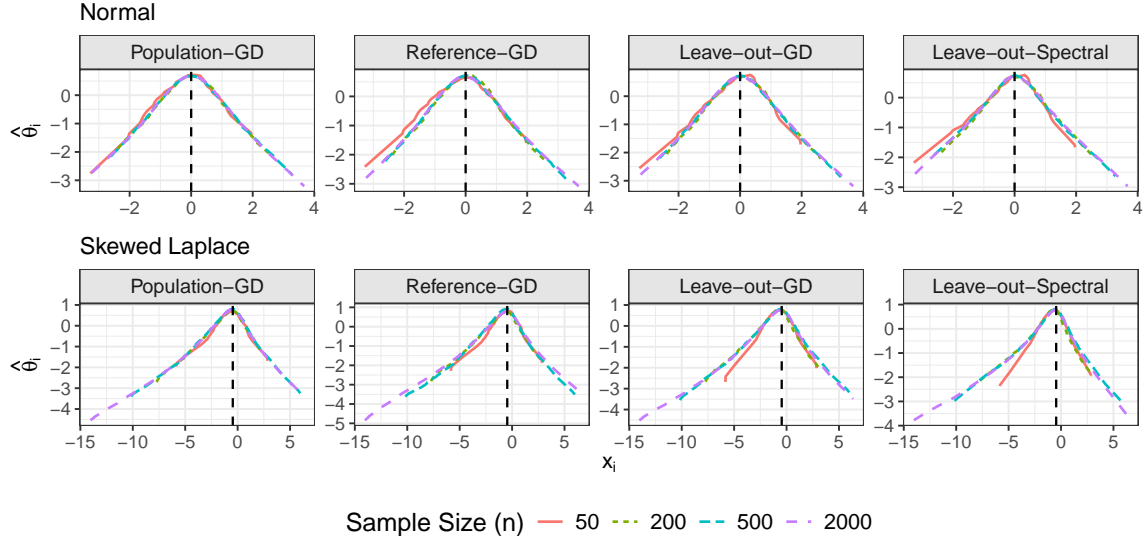


Figure 2: Comparison of the four estimators. Each panel fixes a distribution (Normal or skewed Laplace), and overlays the estimated score curves obtained at sample sizes  $n \in \{50, 200, 500, 2000\}$ . In each panel, the scores  $\hat{\theta}_i$  are plotted against the ordered sample points  $x_{(i)}$ . The vertical dashed line marks the population maximizer  $\mu^* = 0$  for the Normal case and  $\mu^* = -0.462$  for the skewed Laplace case.

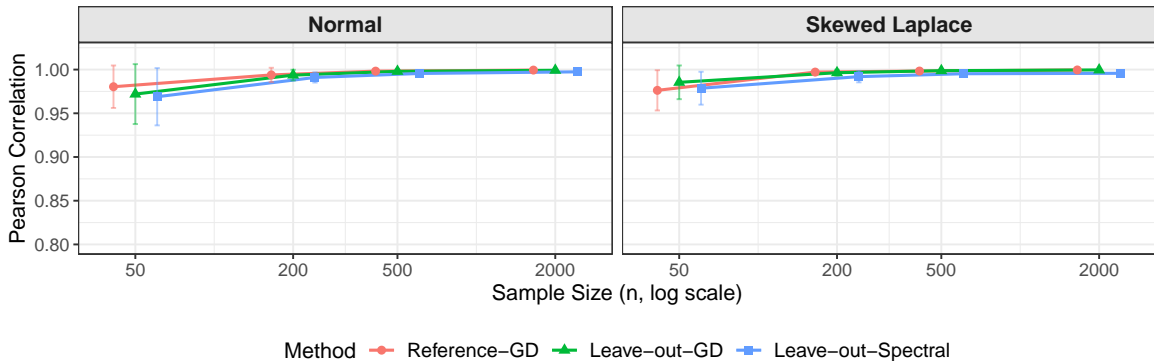


Figure 3: Mean Pearson correlation between the estimated score vectors and the Population-GD benchmark over  $R = 20$  independent replications. Points indicate the mean correlation and vertical error bars denote  $\pm 1$  standard deviation.

Data are generated from three representative distributions: (i) a multivariate Student's  $t$  distribution with  $\nu = 5$  degrees of freedom and identity scatter; (ii) a balanced two-component Gaussian mixture  $0.5 N(u, I_d) + 0.5 N(-u, I_d)$ , where  $u = (4, \dots, 4, 0, \dots, 0)^\top$  has value 4 on the first 10 coordinates; and (iii) a coordinate-wise skewed Laplace model

$\text{ALD}(0, 2, 10)$ , with the first coordinate further scaled by a factor of 100, introducing pronounced skewness and anisotropy.

In each replicate, we construct the leave-two-out pairwise probability matrix  $\{\hat{p}_{ij}^{\text{lto}}\}$  defined in (7). We then compute CORE-GD using Algorithm S.1 (Section S.2), and CORE-Spectral using Algorithm 2. For CORE-GD, we report the centered score vector  $\hat{\boldsymbol{\theta}}$ , while for CORE-Spectral we report the stationary score vector  $\hat{\mathbf{s}}$ .

When  $n > d$ , we compare against four classical depth-based scores: halfspace depth, Mahalanobis depth, projection depth, and spatial depth, all implemented using the `ddalpha` R package (Pokotylo et al., 2019). When  $n < d$ , many classical depth notions become degenerate or computationally infeasible. We therefore include two high-dimensional alternatives: randomized-projection spatial depth (RP-Spatial), which approximates spatial depth via aggregation over random low-dimensional projections (Cuesta-Albertos and Nieto-Reyes, 2008), and the negative  $\ell_2$  distance to the sample mean (Neg-L2).

Performance is evaluated using the Spearman rank correlation between each method's estimated score vector and the benchmark ranking  $(r_F(X_1), \dots, r_F(X_n))$ . Since  $r_F(\cdot)$  has no closed-form expression in general, we approximate  $r_F(X_i)$  by Monte Carlo. Specifically, for each  $y = X_i$ , we draw  $X'_1, \dots, X'_{M_1} \stackrel{\text{i.i.d.}}{\sim} F$  and  $Z_1, \dots, Z_{M_2} \stackrel{\text{i.i.d.}}{\sim} F$ , and compute

$$\hat{r}_F(y) = \frac{1}{M_1 M_2} \sum_{j=1}^{M_2} \sum_{k=1}^{M_1} \mathbb{I}(\|Z_j - X'_k\|_2 > \|Z_j - y\|_2).$$

We take  $M_1 = 2000$  and  $M_2 = 10000$  throughout.

Tables 1 and 2 report the resulting Spearman correlations between each method's score and the Monte Carlo approximation  $\hat{r}_F(X_i)$ . Table 1 summarizes the  $n > d$  settings. Across all distributions and sample sizes, both CORE-GD and CORE-Spectral exhibit consistently high rank agreement with the benchmark, with correlations close to one. The spectral approximation performs comparably to the gradient-based estimator, indicating that it captures the same underlying preference structure while avoiding iterative optimization. In contrast, classical depth-based methods show strong agreement mainly under the elliptically symmetric Student's  $t$  distribution, with substantially weaker concordance under the Gaussian mixture and skewed Laplace models. This behavior is expected, as these depth notions target different population concepts of centrality than the preference-based functional  $r_F(\cdot)$ .

Table 2 presents the results for the  $n < d$  regime. Both CORE estimators continue to

Table 1: Spearman correlation (Mean<sub>SD</sub> over  $R = 20$  replicates) between each method's score and Monte Carlo  $\hat{r}_F(X_i)$  for  $(n, d) \in \{(150, 80), (500, 200)\}$ .

Method	t		Gaussian Mixture		Skewed Laplace	
	(150, 80)	(500, 200)	(150, 80)	(500, 200)	(150, 80)	(500, 200)
CORE-GD	0.999 <sub>0.000</sub>	1.000 <sub>0.000</sub>	0.962 <sub>0.029</sub>	0.989 <sub>0.009</sub>	0.980 <sub>0.013</sub>	0.992 <sub>0.007</sub>
CORE-Spectral	0.996 <sub>0.002</sub>	0.996 <sub>0.001</sub>	0.971 <sub>0.020</sub>	0.990 <sub>0.007</sub>	0.981 <sub>0.013</sub>	0.992 <sub>0.007</sub>
Halfspace	0.800 <sub>0.036</sub>	0.930 <sub>0.009</sub>	0.143 <sub>0.009</sub>	0.222 <sub>0.037</sub>	0.164 <sub>0.121</sub>	0.181 <sub>0.075</sub>
Mahalanobis	0.959 <sub>0.010</sub>	0.989 <sub>0.001</sub>	0.401 <sub>0.066</sub>	0.556 <sub>0.024</sub>	0.073 <sub>0.099</sub>	0.101 <sub>0.049</sub>
Projection	0.945 <sub>0.012</sub>	0.949 <sub>0.007</sub>	0.375 <sub>0.065</sub>	0.306 <sub>0.046</sub>	0.482 <sub>0.068</sub>	0.502 <sub>0.056</sub>
Spatial	0.959 <sub>0.010</sub>	0.989 <sub>0.001</sub>	0.401 <sub>0.067</sub>	0.556 <sub>0.025</sub>	0.073 <sub>0.099</sub>	0.101 <sub>0.049</sub>

Table 2: Spearman correlation (Mean<sub>SD</sub> over  $R = 20$  replicates) between each method's score and Monte Carlo  $\hat{r}_F(X_i)$  for the  $d > n$  settings  $((n, d) \in \{(80, 200), (150, 500)\})$ .

Method	t		Gaussian Mixture		Skewed Laplace	
	(80, 200)	(150, 500)	(80, 200)	(150, 500)	(80, 200)	(150, 500)
CORE-GD	0.999 <sub>0.000</sub>	1.000 <sub>0.000</sub>	0.953 <sub>0.043</sub>	0.961 <sub>0.040</sub>	0.970 <sub>0.024</sub>	0.984 <sub>0.012</sub>
CORE-Spectral	0.990 <sub>0.007</sub>	0.992 <sub>0.008</sub>	0.962 <sub>0.031</sub>	0.970 <sub>0.030</sub>	0.973 <sub>0.020</sub>	0.983 <sub>0.013</sub>
Neg-L2	0.999 <sub>0.000</sub>	1.000 <sub>0.000</sub>	0.786 <sub>0.176</sub>	0.840 <sub>0.140</sub>	0.795 <sub>0.079</sub>	0.739 <sub>0.081</sub>
RP-Spatial	0.989 <sub>0.003</sub>	0.990 <sub>0.003</sub>	0.691 <sub>0.095</sub>	0.579 <sub>0.088</sub>	0.911 <sub>0.064</sub>	0.856 <sub>0.065</sub>

exhibit strong agreement with the benchmark ranking even when the dimension exceeds the sample size. The Neg-L2 baseline performs well primarily under spherical symmetry, consistent with the analysis in Section 3.3.2, but becomes less informative under multimodality and skewness. RP-Spatial partially mitigates high-dimensional degeneracy through random projections, yet still shows reduced agreement relative to CORE in non-elliptical settings. Overall, the results illustrate that CORE maintains stable rank recovery across a wide range of distributional structures and dimensional regimes.

Tables 3 and 4 report Spearman correlations between the estimated scores and the true log-density values  $\log f(X_i)$ . Under the symmetric Student's  $t$  model, CORE is almost perfectly correlated with  $\log f(X_i)$  in both dimensional regimes, consistent with Proposition 2,

Table 3: Spearman correlation (Mean<sub>SD</sub> over  $R = 20$  replicates) between each method's score and the true log-density  $\log f(X_i)$  for  $(n, d) \in \{(150, 80), (500, 200)\}$ .

Method	t		Gaussian Mixture		Skewed Laplace	
	(150, 80)	(500, 200)	(150, 80)	(500, 200)	(150, 80)	(500, 200)
CORE-GD	0.999 <sub>0.000</sub>	1.000 <sub>0.000</sub>	0.622 <sub>0.037</sub>	0.698 <sub>0.030</sub>	0.074 <sub>0.079</sub>	0.087 <sub>0.039</sub>
CORE-Spectral	0.996 <sub>0.001</sub>	0.996 <sub>0.001</sub>	0.629 <sub>0.036</sub>	0.702 <sub>0.030</sub>	0.072 <sub>0.080</sub>	0.083 <sub>0.039</sub>
Halfspace	0.810 <sub>0.032</sub>	0.927 <sub>0.007</sub>	0.141 <sub>0.021</sub>	0.206 <sub>0.044</sub>	0.274 <sub>0.066</sub>	0.238 <sub>0.035</sub>
Mahalanobis	0.961 <sub>0.007</sub>	0.989 <sub>0.001</sub>	0.654 <sub>0.049</sub>	0.749 <sub>0.026</sub>	0.619 <sub>0.049</sub>	0.636 <sub>0.025</sub>
Projection	0.943 <sub>0.014</sub>	0.947 <sub>0.005</sub>	0.475 <sub>0.062</sub>	0.360 <sub>0.031</sub>	0.377 <sub>0.073</sub>	0.306 <sub>0.037</sub>
Spatial	0.961 <sub>0.008</sub>	0.989 <sub>0.001</sub>	0.654 <sub>0.049</sub>	0.749 <sub>0.026</sub>	0.618 <sub>0.049</sub>	0.636 <sub>0.025</sub>

Table 4: Spearman correlation (Mean<sub>SD</sub> over  $R = 20$  replicates) between each method's score and the true log-density  $\log f(X_i)$  for  $(n, d) \in \{(80, 200), (150, 500)\}$ .

Method	t		Gaussian Mixture		Skewed Laplace	
	(80, 200)	(150, 500)	(80, 200)	(150, 500)	(80, 200)	(150, 500)
CORE-GD	0.999 <sub>0.000</sub>	1.000 <sub>0.000</sub>	0.666 <sub>0.057</sub>	0.770 <sub>0.045</sub>	0.119 <sub>0.096</sub>	0.110 <sub>0.063</sub>
CORE-Spectral	0.990 <sub>0.007</sub>	0.992 <sub>0.008</sub>	0.679 <sub>0.062</sub>	0.781 <sub>0.040</sub>	0.117 <sub>0.094</sub>	0.107 <sub>0.064</sub>
Neg-L2	0.999 <sub>0.000</sub>	1.000 <sub>0.000</sub>	0.468 <sub>0.108</sub>	0.636 <sub>0.110</sub>	0.067 <sub>0.106</sub>	0.043 <sub>0.057</sub>
RP-Spatial	0.989 <sub>0.003</sub>	0.990 <sub>0.003</sub>	0.481 <sub>0.085</sub>	0.463 <sub>0.067</sub>	0.101 <sub>0.109</sub>	0.066 <sub>0.059</sub>

which shows that the population score reduces to a radial function of the Mahalanobis distance in the elliptical case. In non-elliptical settings, correlations with  $\log f$  can be substantially lower, reflecting the fact that different procedures target distinct notions of centrality. In particular, CORE is driven by the global geometry induced by the Euclidean dissimilarity, whereas  $\log f$  represents a local quantity that is sensitive to multimodality, skewness, and anisotropic scaling.

## 5 Conclusion and Discussion

We proposed CORE, a preference-based framework for defining population centrality through reference-based pairwise comparisons on a general dissimilarity space  $(\mathcal{X}, \delta)$ . By projecting the induced pairwise preference structure onto a one-dimensional BTL score, CORE aggregates local comparison information into a globally interpretable ranking. A central conceptual contribution of this work is the population functional  $r_F(\cdot)$ , which provides an intrinsic notion of preference-based centrality that is defined independently of any parametric scoring model. Because  $r_F(\cdot)$  depends explicitly on the chosen dissimilarity  $\delta$ , the framework offers a flexible mechanism for tailoring centrality to the geometry and semantics of the problem at hand.

On the methodological side, we developed two complementary estimators. The optimization-based estimator, CORE-GD, solves the empirical M-projection via first-order constrained optimization and yields calibrated scores with strong statistical and numerical stability. To address scalability concerns, we also introduced CORE-Spectral, a fast spectral approximation based on a Markov chain construction, which retains the essential ranking structure while significantly reducing computational cost. Our theoretical analysis establishes existence, uniqueness, and intrinsic monotonicity of the population target, and shows that the induced score satisfies the canonical axioms of statistical depth under mild regularity conditions.

Throughout the paper, we focused on the no-tie formulation, which is natural for continuous distributions where ties occur with probability zero. When ties are relevant, for example under discrete metrics or quantized representations, standard tie corrections can be incorporated by assigning half weight to equality events in the pairwise comparison rule. Such modifications require only minor technical adjustments and do not alter the conceptual framework.

Several limitations merit discussion. First, empirical estimation of pairwise preferences is inevitably affected by comparison noise and finite-sample bias, which may induce ranking variability in challenging regimes such as weak signal, heavy tails, or high-dimensional settings. Second, the full pairwise construction entails  $O(n^2)$  time and memory costs, which can become prohibitive for very large sample sizes despite the availability of spectral approximations.

These limitations point to several promising directions for future work. From a modeling perspective, an important extension is to develop adaptive or data-driven strategies for selecting or learning the dissimilarity  $\delta$  so that the resulting preference-based centrality aligns more closely with downstream objectives. Another direction is to study smoother or probabilistic comparison rules that reduce sensitivity to small distance perturbations when  $\delta$  is noisy or approximately computed. From a computational standpoint, scalable variants based on sparse comparison graphs, pair subsampling, and stochastic or mini-batch optimization schemes are natural avenues to pursue. Finally, developing principled uncertainty quantification tools—including confidence intervals and hypothesis tests for scores and induced rankings—and exploring richer paired-comparison models beyond the BTL projection remain important open problems for preference-based centrality and ranking.

## References

Bradley, R. A. and M. E. Terry (1952). Rank analysis of incomplete block designs: I. the method of paired comparisons. *Biometrika* 39, 324–345.

Chaudhuri, P. (1996). On a geometric notion of quantiles for multivariate data. *Journal of the American Statistical Association* 91(434), 862–872.

Cuesta-Albertos, J. A. and A. Nieto-Reyes (2008). The random tukey depth. *Computational Statistics & Data Analysis* 52(11), 4979–4988.

Deb, N. and B. Sen (2023). Multivariate rank-based distribution-free nonparametric testing using measure transportation. *Journal of the American Statistical Association* 118(541), 192–207.

Feldbauer, R. and A. Flexer (2019). A comprehensive empirical comparison of hubness reduction in high-dimensional spaces. *Knowledge and Information Systems* 59(1), 137–166.

Hallin, M. and D. Paindaveine (2002). Optimal tests for multivariate location based on interdirections and pseudo-mahalanobis ranks. *The Annals of Statistics* 30(4), 1103–1133.

Hallin, M. and D. Paindaveine (2006). Parametric and semiparametric inference for shape:

the role of the scale functional. *Statistics & Decisions* 24(3), 327–350.

Hallin, M. and M. L. Puri (1995). A multivariate wald-wolfowitz rank test against serial dependence. *Canadian Journal of Statistics* 23(1), 55–65.

Liu, R. Y. (1990). On a notion of data depth based on random simplices. *The Annals of Statistics* 18(1), 405–414.

Liu, R. Y. and K. Singh (1993). A quality index based on data depth and multivariate rank tests. *Journal of the American Statistical Association* 88(421), 252–260.

Luce, R. D. (1959). *Individual Choice Behavior*, Volume 4. Wiley New York.

Negahban, S., S. Oh, and D. Shah (2017). Rank centrality: Ranking from pairwise comparisons. *Operations Research* 65(1), 266–287.

Oja, H. (2010). *Multivariate nonparametric methods with R: an approach based on spatial signs and ranks*. Springer Science & Business Media.

Pan, W., Y. Tian, X. Wang, and H. Zhang (2018). Ball divergence: nonparametric two sample test. *Annals of Statistics* 46(3), 1109.

Parzen, E. (1962). On estimation of a probability density function and mode. *The Annals of Mathematical Statistics* 33(3), 1065–1076.

Pokotylo, O., P. Mozharovskyi, and R. Dyckerhoff (2019). Depth and depth-based classification with R package ddalpha. *Journal of Statistical Software* 91(5), 1–46.

Puri, M. L. and P. K. Sen (1966). On a class of multivariate multisample rank-order tests. *Sankhyā: The Indian Journal of Statistics, Series A (1961–2002)* 28(4), 353–376.

Radovanovic, M., A. Nanopoulos, and M. Ivanovic (2010). Hubs in space: Popular nearest neighbors in high-dimensional data. *Journal of Machine Learning Research* 11(sept), 2487–2531.

Tukey, J. W. (1974). Mathematics and the picturing of data. In *Proceedings of the International Congress of Mathematicians*, Volume 2, pp. 523–531. Vancouver.

Vardi, Y. and C.-H. Zhang (2000). The multivariate  $L_1$ -median and associated data depth. *Proceedings of the National Academy of Sciences* 97(4), 1423–1426.

Vu, M. D., M. Liu, and D. Zhou (2025). A trainable centrality framework for modern data.

Zhou, D. and H. Chen (2023). A new ranking scheme for modern data and its application to two-sample hypothesis testing. In *Proceedings of Thirty Sixth Conference on Learning Theory*, Volume 195 of *Proceedings of Machine Learning Research*, pp. 3615–3668. PMLR.

Zuo, Y. (2003). Projection-based depth functions and associated medians. *The Annals of Statistics* 31(5), 1460–1490.

Zuo, Y. and R. Serfling (2000). General notions of statistical depth function. *The Annals of Statistics* 28(2), 461–482.